

REFERENCES

- [1] M. K. Simon and M. S. Alouini, *Digital Communications Over Fading Channels*. New York: Wiley-Interscience, 2000.
- [2] M. O. Hasna and M. S. Alouini, "Outage probability of multi-hop transmission over Nakagami fading channels," *IEEE Commun. Lett.*, vol. 7, no. 5, pp. 216–218, May 2003.
- [3] G. Farhadi and N. C. Beaulieu, "On the ergodic capacity of multi-hop wireless relaying systems," *IEEE Trans. Wireless Commun.*, vol. 8, no. 5, pp. 2286–2291, May 2009.
- [4] G. Farhadi and N. C. Beaulieu, "Capacity of amplify-and-forward multi-hop relaying systems under adaptive transmission," *IEEE Trans. Commun.*, to be published.
- [5] M. O. Hasna and M. S. Alouini, "End-to-end performance of transmission systems with relays over Rayleigh fading channels," *IEEE Trans. Wireless Commun.*, vol. 2, no. 6, pp. 1126–1131, Nov. 2003.
- [6] J. Boyer, D. D. Falconer, and H. Yanikomeroglu, "Multi-hop diversity in wireless relaying channels," *IEEE Trans. Commun.*, vol. 52, no. 10, pp. 1820–1830, Oct. 2004.
- [7] M. O. Hasna and M. S. Alouini, "Harmonic mean and end-to-end performance of transmission systems with relays," *IEEE Trans. Commun.*, vol. 52, no. 1, pp. 130–135, Jan. 2004.
- [8] M. O. Hasna and M. S. Alouini, "A performance study of dual-hop transmissions with fixed gain relays," *IEEE Trans. Wireless Commun.*, vol. 3, no. 6, pp. 1963–1968, Nov. 2004.
- [9] G. K. Karagiannidis, T. A. Tsiftsis, and R. K. Mallik, "Bounds for multihop relayed communications in Nakagami- m fading," *IEEE Trans. Commun.*, vol. 54, no. 1, pp. 18–22, Jan. 2006.
- [10] G. K. Karagiannidis, "Performance bounds of multihop wireless communications with blind relays over generalized fading channels," *IEEE Trans. Wireless Commun.*, vol. 5, no. 3, pp. 498–503, Mar. 2006.
- [11] M. Di Renzo, F. Graziosi, and F. Santucci, "On the performance of CSI-assisted cooperative communications over generalized fading channels," in *Proc. IEEE ICC*, May 2008, pp. 1001–1007.
- [12] G. Farhadi and N. C. Beaulieu, "On the performance of amplify-and-forward cooperative links with fixed gain relays," *IEEE Trans. Wireless Commun.*, vol. 7, no. 5, pp. 1851–1856, May 2008.
- [13] I. S. Gradshteyn and I. M. Ryzhik, *Table of Integrals, Series, and Products*, 6th ed. New York: Academic, 2000.
- [14] K. Cho and D. Yoon, "On the general BER expression of one- and two-dimensional amplitude modulations," *IEEE Trans. Commun.*, vol. 50, no. 7, pp. 1074–1080, Jul. 2002.
- [15] G. M. Dillard, "Recursive computation of the generalized Q -function," *IEEE Trans. Aerosp. Electron. Syst.*, vol. AES-50, no. 9, pp. 614–615, Jul. 1973.
- [16] J. N. Laneman, D. N. C. Tse, and G. W. Wornell, "Cooperative diversity in wireless networks: Efficient protocols and outage behavior," *IEEE Trans. Inf. Theory*, vol. 50, no. 12, pp. 3062–3080, Dec. 2004.
- [17] M. Abramowitz and I. A. Stegun, *Handbook of Mathematical Functions With Formulas, Graphs, and Mathematical Tables*, 7th ed. New York: Dover, 1972.

Maximum-Throughput Irregular Distributed Space-Time Code for Near-Capacity Cooperative Communications

Lingkun Kong, Soon Xin Ng, Robert G. Maunder, and Lajos Hanzo

Abstract—This paper presents an irregular distributed space-time (Ir-DST) coding scheme designed for near-capacity cooperative communications where the system's effective throughput is also maximized with the aid of a joint source-and-relay mode design procedure. At the source node, a serially concatenated scheme comprising an Irregular Convolutional Code (IRCC), a recursive unity-rate code (URC), and a space-time block code (STBC) was designed for the sake of approaching the corresponding source-to-relay link capacity, where the IRCC was optimized with the aid of EXtrinsic Information Transfer (EXIT) charts. At the relay node, another IRCC is serially concatenated with an identical STBC. Before transmitting the relayed information, the relay's IRCC is reoptimized based on EXIT chart analysis for the sake of approaching the relay channel's capacity and to maximize the relay's coding rate, which results in a maximized effective throughput. We will demonstrate that the topology of the Ir-DST system coincides with that of a distributed turbo code (DTC). At the destination node, a novel three-stage iterative decoding scheme is constructed to achieve decoding convergence to an infinitesimally low bit-error ratio (BER). Finally, our numerical results show the proficiency of our joint source-and-relay mode design procedure, demonstrating that the proposed Ir-DST coding scheme is capable of near-capacity cooperative communications and of maximizing the effective throughput.

Index Terms—EXtrinsic Information Transfer (EXIT) charts, irregular distributed space-time (Ir-DST) code, iterative detection.

I. INTRODUCTION

Over the past few years, cooperative communication schemes [1]–[3], which combine the benefits of distributed multiple-input–multiple-output (MIMO) systems with relay technologies, have intensively been studied. In a relay network, where the nodes (users) are equipped with either single or multiple antennas, cooperative communications allow the nodes (users) to assist each other in forwarding (relay) all messages to the destination rather than transmitting only their own messages. Since the MIMO transmitter's elements in such a network are distributed, the network forms a "distributed MIMO" system. For the sake of improving the diversity gain of relay-aided networks, numerous cooperative protocols [1]–[4] have been proposed. In most cooperative scenarios, the decode-and-forward (DF) and amplify-and-forward (AF) protocols are predominantly used. However, a strong channel code is required to mitigate the potential error propagation in the DF scheme or to avoid noise enhancement in the AF scheme.

Inspired by the classic turbo codes used in noncooperative communication scenarios, distributed turbo codes (DTCs) [5] have been proposed for "distributed MIMO" systems, which benefit from a *turbo processing* gain. However, DTCs suffer from having an imperfect communication link between the source and relay nodes. Hence, a three-component distributed turbo trellis-coded modulation (DTTCM) scheme has been proposed in [6], which takes into consideration the realistic condition of having an imperfect source-to-relay communication link. The DTTCM scheme [6], designed using EXtrinsic

Manuscript received May 7, 2009; revised November 17, 2009. First published January 15, 2010; current version published March 19, 2010. This work was supported in part by the China–U.K. Scholarship Council, by the Engineering and Physical Sciences Research Council U.K., and by the European Union, under the auspices of the Optimix project. The review of this paper was coordinated by Dr. A. Ghayeb.

The authors are with the School of Electronics and Computer Science, University of Southampton, SO17 1BJ Southampton, U.K. (e-mail: lk06r@ecs.soton.ac.uk; sxn@ecs.soton.ac.uk; rm@ecs.soton.ac.uk; lh@ecs.soton.ac.uk).

Digital Object Identifier 10.1109/TVT.2010.2040398

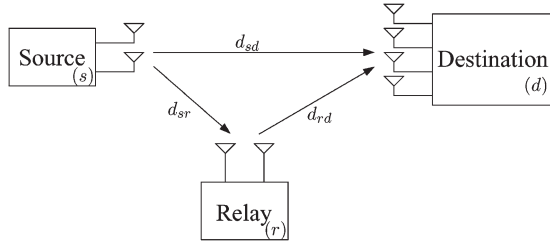


Fig. 1. Schematic of a single relay-aided multi-antenna system, where d_{ab} is the geographical distance between nodes a and b .

Information Transfer (EXIT) chart analysis [7], [8], is capable of minimizing the decoding error probability at the relay node and performs close to its idealized counterpart that assumes perfect decoding at the relay node. However, the DTTCCM of [6] still fails to approach the corresponding relay channel's capacity.

On the other hand, there exist several capacity-approaching turbo coding schemes designed for specific network topologies proposed by Zhang and Duman [9] for half-duplex relay systems, where the authors did not aim to propose a general design procedure to find the optimal coding schemes under different relay-network configurations. Against this background, our objective here is to design a near-capacity cooperative scheme using a joint source-and-relay mode design procedure, which is suitable for arbitrary relay-network configurations. Furthermore, the relay system's effective throughput is maximized as a benefit of the proposed design procedure. For the sake of approaching the relay channel's capacity, we first derive the theoretical lower and upper bounds on the Continuous-input–Continuous-output Memoryless Channel (CCMC) [10], [11] capacity and the Discrete-input Continuous-output Memoryless Channel (DCMC) [10], [11] capacity (constrained information rate) with independent and uniformly distributed (i.u.d.) inputs. A new Irregular Distributed Space-Time (Ir-DST) coding scheme is proposed, where two Irregular Convolutional Codes (IRCCs) [12], [13] having different IRCC weighting coefficients are employed at the source and relay nodes, respectively, which are designed to support near-capacity cooperative communications.

The rest of this paper is organized as follows: The system model is described in Section II. Section III specifies the encoding and decoding processes of the novel Ir-DST coding scheme. The relay channel's capacity computation and the EXIT-chart-aided joint source-and-relay mode design are detailed in Section IV, whereas our simulation results and discussions are provided in Section V. Finally, we conclude in Section VI.

II. SYSTEM MODEL

We consider a two-hop relay-aided network, which has a single source node having N_s antennas, a single relay node equipped with N_r antennas, and a destination node having N_d antennas, where all nodes obey the half-duplex constraint, i.e., a node cannot simultaneously transmit and receive. The schematic of the proposed system is shown in Fig. 1, which typically entails two phases. In *Phase I*, the source node s broadcasts the information to both the relay node r and the destination node d . The relay node r processes the received information and forwards it to the destination node d in *Phase II*, whereas the source node s remains silent. The destination performs decoding based on the messages it received in both phases. As in [14], we model the communication links in Fig. 1 as being subjected to both long-term free-space path loss and short-term uncorrelated Rayleigh fading.

Let d_{ab} and P_{ab} denote the geometrical distance and the path loss between nodes a and b . The path loss and the geometrical distance can be related by [14]

$$P_{ab} = \frac{K}{d_{ab}^\alpha} \quad (1)$$

where K is a constant that depends on the environment, and α is the path-loss exponent. For a free-space scenario, we have $\alpha = 2$. The relationship between the energy E_{sr} received at the relay node and that at the destination node E_{sd} can be expressed as

$$E_{sr} = \frac{P_{sr}}{P_{sd}} E_{sd} = G_{sr} E_{sd} \quad (2)$$

where G_{sr} is the power gain (or geometrical gain) [14] experienced by the source-to-relay link with respect to the source-to-destination link as a benefit of the commensurately reduced distance and path loss, which can be expressed as

$$G_{sr} = \left(\frac{d_{sd}}{d_{sr}} \right)^2. \quad (3)$$

Similarly, the geometrical gain at the relay-to-destination link with respect to the source-to-destination link can be formulated as

$$G_{rd} = \left(\frac{d_{sd}}{d_{rd}} \right)^2. \quad (4)$$

Naturally, the geometrical gain at the source-to-destination link with respect to itself is unity, i.e., $G_{sd} = 1$. Therefore, owing to the triangle inequality applied in Fig. 1, the geometrical gains G_{sr} and G_{rd} have to satisfy

$$G_{sr} + G_{rd} + 2\sqrt{G_{sr}G_{rd}} \geq G_{sr}G_{rd}. \quad (5)$$

We assume that the relay node is closer to the source node than to the destination node, whereas both the source and the relay are far from the destination, i.e., we have $G_{sr} > G_{rd}$. In this scenario, the relay benefits from a higher received signal power than the destination. This assumption facilitates the employment of near-perfect DF relaying (similar arguments can be found in [15] and [16]); otherwise, other relaying modes might be better choices [e.g., AF and compress-and-forward]. Hence, the vector hosting the received signal at the relay node during *Phase I*, which consists of L_s number of symbol periods, can be formulated as

$$\mathbf{y}_r = \sqrt{G_{sr}} \mathbf{H}_{sr} \mathbf{c}_s + \mathbf{n}_r \quad (6)$$

where $\mathbf{y}_r = [y_{r,1}, \dots, y_{r,N_r}]^T$ is the N_r -element vector of the received signals at the relay node, and \mathbf{H}_{sr} is the $(N_r \times N_s)$ -element channel matrix, the entries of which are independent and identically complex Gaussian distributed with a zero mean and a variance of 0.5 per dimension. Furthermore, $\mathbf{c}_s = [c_{s,1}, \dots, c_{s,N_s}]^T$ is an N_s -element vector of the signals transmitted from the source node at an average power of P_0 , and $\mathbf{n}_r = [n_{r,1}, \dots, n_{r,N_r}]^T$ is an N_r -element noise vector. Each element of \mathbf{n}_r is an additive white Gaussian noise (AWGN) process having a zero mean and a variance of $N_0/2$ per dimension. By contrast, the signal vector received at the destination node during *Phase I* can be expressed as

$$\mathbf{y}_d^I = \sqrt{G_{sd}} \mathbf{H}_{sd} \mathbf{c}_s + \mathbf{n}_d \quad (7)$$

and the signal vector received at the destination node during *Phase II*, when L_r number of symbols are transmitted from the relay node, is formulated as

$$\mathbf{y}_d^{II} = \sqrt{G_{rd}} \mathbf{H}_{rd} \mathbf{c}_r + \mathbf{n}_d \quad (8)$$

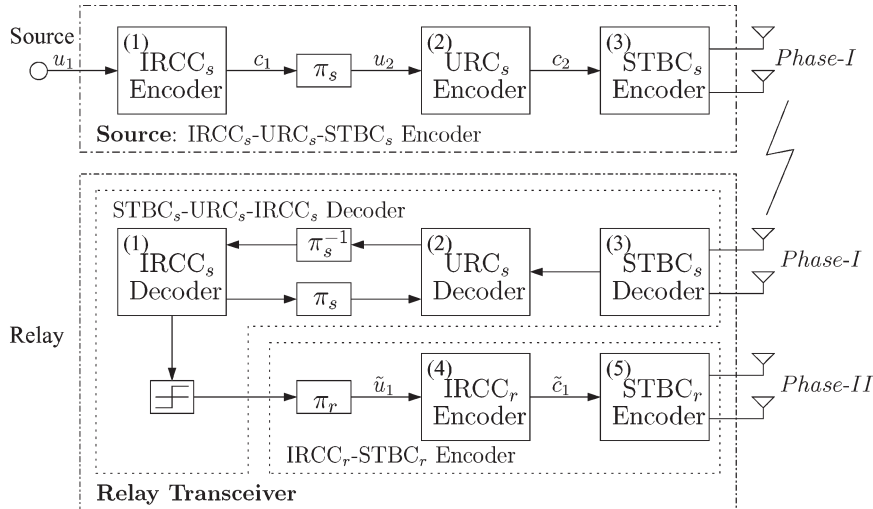


Fig. 2. Schematic of the Ir-DST encoder.

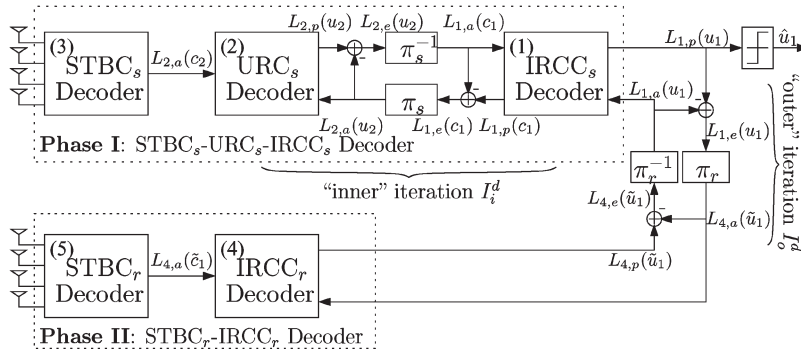


Fig. 3. Three-stage iterative decoder of the Ir-DST coding scheme.

where $\mathbf{y}_d^I = [y_{d,1}^I, \dots, y_{d,N_d}^I]^T$ and $\mathbf{y}_d^{II} = [y_{d,1}^{II}, \dots, y_{d,N_d}^{II}]^T$ are both N_d -element vectors of the signals received during *Phase I* and *Phase II* at the destination node, respectively, and $\mathbf{H}_{sd} \in \mathbb{C}^{N_d \times N_s}$ and $\mathbf{H}_{rd} \in \mathbb{C}^{N_d \times N_r}$ are the corresponding channel matrices, the entries of which are independent and identically complex Gaussian distributed with a zero mean and a variance of 0.5 per dimension. Finally, $\mathbf{c}_r = [c_{r,1}, \dots, c_{r,N_r}]^T$ is an N_r -element vector of the signals transmitted from the relay node at the same power P_0 as that of \mathbf{c}_s , and $\mathbf{n}_d = [n_{d,1}, \dots, n_{d,N_d}]^T$ is an N_d -element AWGN vector, with each element having a zero mean and a variance of $N_0/2$ per dimension.

III. IRREGULAR DISTRIBUTED SPACE TIME CODES

A. Ir-DST Encoder

In this paper, we consider a specific two-hop relay-aided network associated with $N_s = 2$, $N_r = 2$, and $N_d = 4$, as shown in Fig. 1. At the source node, we use Alamouti's space-time block code (STBC) [17] amalgamated with a recursive unity-rate code (URC)¹ used as the inner code, whereas an IRCC [12], [13] having an average code rate of R_s is employed as the outer code, which is optimized with the aid of EXIT chart analysis for the sake of near-error-free decoding at channel signal-to-noise ratios (SNRs) close to the capacity of the source-to-relay link at the relay node during the relay's receive period of *Phase I*.

¹URCs were proposed by Divsalar *et al.* [18] for the sake of extending the overall system's impulse response to an infinite duration, which efficiently spreads the extrinsic information and, hence, improves the achievable iterative detection gain.

On the other hand, as shown in Fig. 2, in the relay's transmit period of *Phase II*, another IRCC having a code rate of R_r is amalgamated with Alamouti's STBC scheme, where the IRCC is further improved with the aid of a joint source-and-relay mode design procedure, as we will show in Section IV-B for the sake of approaching the relay channel's capacity. Specifically, the notations π_s and π_r in Fig. 2 represent the bitwise random interleaver used at the source node and the relay node, respectively. Compared with the topology of the DTC [5], it may be observed that the cooperative scheme seen in Fig. 2 combines the benefits of a serially concatenated scheme and a DTC, which is referred to as an Ir-DST coding scheme in this contribution.

B. Three-Stage Iterative Decoding at the Destination

The novel three-stage iterative decoder structure of the Ir-DST scheme is shown in Fig. 3. At the destination node, the signals received during *Phase I* are first decoded by the amalgamated² "STBC_s-URC_s" decoder to produce the *a priori* log-likelihood ratio (LLR) values $L_{1,a}(c_1)$ of the coded bits c_1 by the maximum *a posteriori* probability algorithm [19]. The IRCC_s decoder shown in the top right of Fig. 3 processes the information forwarded by the "STBC_s-URC_s" decoder in conjunction with the *a priori* LLR values $L_{1,a}(u_1)$ of the information bits u_1 gleaned by the "STBC_r-IRCC_r" relay decoder to generate the *a posteriori* LLR values $L_{1,p}(u_1)$ and $L_{1,p}(c_1)$ of the information bits u_1 and of the coded bits c_1 , respectively. As shown in Fig. 3, the *a priori* LLRs $L_{1,a}(c_1)$ are subtracted from the

²The terminology "amalgamated" is used here to indicate that, although it might have some benefits to exchange extrinsic information between these two blocks, no iterations were used between them.

a posteriori LLR values $L_{1,p}(c_1)$, and then, they are fed back to the “STBC_s-URC_s” decoder as the *a priori* information $L_{2,a}(u_2)$ through the interleaver π_s . We term this information-exchange process seen in the top trace in Fig. 3 as the “inner” iteration.³ Similarly, during the “outer” iterations, the *a priori* LLR values $L_{1,a}(u_1)$ fed into the IRCC_s decoder are also subtracted from the *a posteriori* LLR values $L_{1,p}(u_1)$ for the sake of generating the extrinsic LLR values $L_{1,e}(u_1)$, as shown in the top right corner of Fig. 3. Then, $L_{1,e}(u_1)$ is passed to the amalgamated “STBC_r-IRCC_r” relay decoder as the *a priori* information $L_{4,a}(\tilde{u}_1)$ through the interleaver π_r in conjunction with the signals received during *Phase II* to compute the *a posteriori* LLR values $L_{4,p}(\tilde{u}_1)$ of the permuted information bits \tilde{u}_1 from the relay node. As shown in Fig. 3, the extrinsic information $L_{4,e}(\tilde{u}_1)$ is generated by subtracting the *a priori* information $L_{4,a}(\tilde{u}_1)$ from the *a posteriori* information $L_{4,p}(\tilde{u}_1)$ before $L_{4,e}(\tilde{u}_1)$ is fed back to the IRCC_s decoder as the *a priori* information $L_{1,a}(u_1)$ through the de-interleaver π_r^{-1} . During the last “outer” iteration, only the LLR values $L_{1,p}(u_1)$ of the original information bits u_1 are required, which are passed to the hard-decision block in Fig. 3 to estimate the source bits.

IV. NEAR-CAPACITY SYSTEM DESIGN AND ANALYSIS

To design a near-capacity coding scheme for the proposed two-hop relay-aided network, in Section IV-A, we first derive the upper and lower bounds on the relay channel’s CCMC capacity and those of the DCMC capacity (constrained information rate) for Alamouti’s STBC scheme since the relay channel’s exact capacity formula is unavailable. Then, the EXIT-chart-based joint source-and-relay mode design will be carried out in Section IV-B.

A. Relay Channel’s Capacity

As presented in [15], a general upper bound on the CCMC capacity of a half-duplex⁴ relay system may be derived based on the original results of [20] on the full-duplex relay channels, which is given by

$$C_{\text{CCMC}}^{\text{coop}} \leq \max_{p(x_1, x_2, x)} \min \{ \lambda E [I(X_1 Y_1, Y)] + (1 - \lambda) E [I(X_2 Y_2 | X)] + \lambda E [I(X_1 Y_1)] + (1 - \lambda) E [I(X_2, X Y_2)] \} \quad (9)$$

where λ is the ratio of the first time slot duration to the total frame duration. On the other hand, another achievable rate definition for the DF protocol, which can be regarded as a lower bound on the CCMC capacity of the relay system, was provided in [15] in the form of

$$C_{\text{CCMC}}^{\text{coop}} \geq \max_{p(x_1, x_2, x)} \min \{ \lambda E [I(X_1 Y)] + (1 - \lambda) E [I(X_2 Y_2 | X)] + \lambda E [I(X_1 Y_1)] + (1 - \lambda) E [I(X_2, X Y_2)] \} \quad (10)$$

³Explicitly, at the destination node, the extrinsic information exchange between the amalgamated “STBC_s-IRCC_s” decoder and the IRCC_s decoder is referred to as the “inner” iteration, whereas that between the parallel amalgamated “STBC_s-URC_s-IRCC_s” decoder and the amalgamated “STBC_r-IRCC_r” relay decoder is referred to as the “outer” iteration.

⁴In [15], the source node continues transmission during the second time slot.

where $p(x_1, x_2, x)$ indicates the joint probability of the signals transmitted from the source and relay nodes. The signals X_1 and X_2 are transmitted from the source node during the first and the second time slot, respectively, whereas Y_1 and Y_2 represent the corresponding signals received at the destination during the two consecutive time slots. Furthermore, X and Y are the transmitted and received signals at the relay node, respectively.

In our half-duplex-constrained relay-aided system, the source node does not transmit during *Phase II*, i.e., $X_2 = 0$, and we have $E[I(X_2; Y_2 | X)] = 0$ and $E[I(X_2, X; Y_2)] = E[I(X; Y_2)]$ in (9) and (10). Hence, based on (6)–(8), the upper and lower bounds of the relay channel’s capacity can be derived accordingly as

$$C_{\text{CCMC}}^{\text{coop}} \leq \max_{p(c_s, c_r)} \min \left\{ \frac{L_s}{L_s + L_r} E [I(C_s Y_d^I, Y_r)] + \frac{L_s}{L_s + L_r} E [I(C_s Y_d^I)] + \frac{L_r}{L_s + L_r} E [I(C_r Y_d^{II})] \right\} \quad (11)$$

$$C_{\text{CCMC}}^{\text{coop}} \geq \max_{p(c_s, c_r)} \min \left\{ \frac{L_s}{L_s + L_r} E [I(C_s Y_r)] + \frac{L_s}{L_s + L_r} E [I(C_s Y_d^I)] + \frac{L_r}{L_s + L_r} E [I(C_r Y_d^{II})] \right\} \quad (12)$$

respectively.

In addition to the CCMC capacity bounds of (11) and (12), we evaluate the information-rate bounds for the relaying channel in conjunction with i.u.d. inputs. In this contribution, we employ Alamouti’s G2 scheme [17] at both the source and relay nodes, whose *codeword* matrix is given by

$$\mathbf{C}_{G2} = \begin{pmatrix} c_1 & c_2 \\ -\bar{c}_2 & \bar{c}_1 \end{pmatrix}^T. \quad (13)$$

Based on (6)–(8), the signal received at the relay node during $V = 2$ consecutive symbol periods can be written as

$$\mathbf{Y}_r = \sqrt{G_{sr}} \mathbf{H}_{sr} \mathbf{C}_s + \mathbf{N}_r \quad (14)$$

while the signals received at the destination node during $V = 2$ consecutive symbol periods in *Phase I* and *Phase II* are expressed as

$$\mathbf{Y}_d^I = \sqrt{G_{sd}} \mathbf{H}_{sd} \mathbf{C}_s + \mathbf{N}_d \quad (15)$$

$$\mathbf{Y}_d^{II} = \sqrt{G_{rd}} \mathbf{H}_{rd} \mathbf{C}_r + \mathbf{N}_d \quad (16)$$

respectively. Specifically, $\mathbf{Y}_r = [\mathbf{y}_{r,1}, \dots, \mathbf{y}_{r,V}] \in \mathbb{C}^{N_r \times V}$, $\mathbf{Y}_d^I = [\mathbf{y}_{d,1}^I, \dots, \mathbf{y}_{d,V}^I] \in \mathbb{C}^{N_d \times V}$, and $\mathbf{Y}_d^{II} = [\mathbf{y}_{d,1}^{II}, \dots, \mathbf{y}_{d,V}^{II}] \in \mathbb{C}^{N_d \times V}$ are the matrices hosting the sampled signal received at the relay node and the destination node, respectively, whereas $\mathbf{H}_{sr} \in \mathbb{C}^{N_r \times N_s}$, $\mathbf{H}_{sd} \in \mathbb{C}^{N_d \times N_s}$, and $\mathbf{H}_{rd} \in \mathbb{C}^{N_d \times N_r}$ are the corresponding quasi-static channel matrices, which are constant over $V = 2$ consecutive symbol periods. Furthermore, $\mathbf{C}_s = [\mathbf{c}_{s,1}, \dots, \mathbf{c}_{s,V}] \in \mathbb{C}^{N_s \times V}$ and $\mathbf{C}_r = [\mathbf{c}_{r,1}, \dots, \mathbf{c}_{r,V}] \in \mathbb{C}^{N_r \times V}$ represent Alamouti’s G2 matrices characterizing the transmissions of the source and relay nodes, whereas $\mathbf{N}_r = [\mathbf{n}_{r,1}, \dots, \mathbf{n}_{r,V}] \in \mathbb{C}^{N_r \times V}$ and $\mathbf{N}_d = [\mathbf{n}_{d,1}, \dots, \mathbf{n}_{d,V}] \in \mathbb{C}^{N_d \times V}$ represent the AWGN matrix incurred at the relay and destination nodes, respectively.

Hence, we may readily derive the upper and lower bounds on the constrained information rate of the relaying channel with i.u.d.

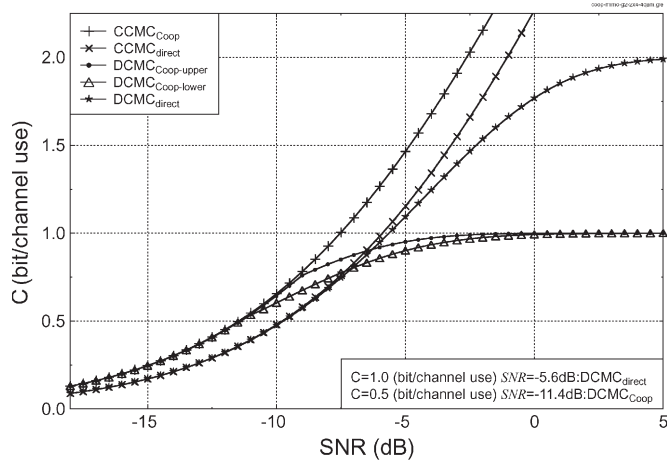


Fig. 4. Relay channel's CCMC capacity and constrained information-rate bounds employing the 4QAM-modulated G2 scheme when the network is configured with $G_{sr} = 8$ and $G_{rd} = 2$, and $L_s = L_r$.

G2 codeword-matrix inputs as

$$C_{\text{DCMC}}^{\text{coop-g2}} \leq \min \left\{ \frac{L_s}{L_s + L_r} E [I(\mathbf{C}_s \mathbf{Y}_d^I, \mathbf{Y}_r)] \right. \\ \left. \frac{L_s}{L_s + L_r} E [I(\mathbf{C}_s \mathbf{Y}_d^I)] \right. \\ \left. + \frac{L_r}{L_s + L_r} E [I(\mathbf{C}_r \mathbf{Y}_d^{II})] \right\} \quad (17)$$

$$C_{\text{DCMC}}^{\text{coop-g2}} \geq \min \left\{ \frac{L_s}{L_s + L_r} E [I(\mathbf{C}_s \mathbf{Y}_r)] \right. \\ \left. \frac{L_s}{L_s + L_r} E [I(\mathbf{C}_s \mathbf{Y}_d^I)] \right. \\ \left. + \frac{L_r}{L_s + L_r} E [I(\mathbf{C}_r \mathbf{Y}_d^{II})] \right\} \quad (18)$$

respectively, where the corresponding constrained information rates of $E[I(\mathbf{C}_s; \mathbf{Y}_d^I, \mathbf{Y}_r)]$, $E[I(\mathbf{C}_s; \mathbf{Y}_r)]$, $E[I(\mathbf{C}_s; \mathbf{Y}_d^I)]$, and $E[I(\mathbf{C}_r; \mathbf{Y}_d^{II})]$ can be computed based on [21, eq. (9)].

An example for a specific network configuration associated with $L_s = L_r$, $G_{sr} = 8$, and $G_{rd} = 2$ is shown in Fig. 4, where the direct-transmission-based benchmark is also depicted with the power constraint P_0 for a fair comparison. The CCMC capacity and the information rates obeying the i.u.d. four-state quadrature amplitude modulation (4QAM)-modulated G2 codeword-matrix-input constraint are evaluated by the upper and lower bounds given in (11) and (12), and (17) and (18), respectively. We can see in Fig. 4 that the lower and upper bounds converge and exhibit a substantial capacity gain over conventional direct transmission in the low and medium SNR regimes below a certain convergence threshold, which is caused by the geometrical gain of the relay-to-destination link. On the other hand, it is observed that the relay channel's DCMC capacity is only half of the direct transmission due to a factor of $(L_r/L_s + L_r) = 0.5$ multiplexing loss in the half-duplex scenario. The DCMC capacity provides the fundamental limits on the performance of a practical coding/decoding scheme. In Section IV-B, we will propose an optimal distributed coding scheme, which is capable of approaching the relay channel's limits under arbitrary relay network configuration.

B. Joint Code Design for the Source-and-Relay Nodes Based on EXIT Charts

For the sake of analyzing the convergence behaviors of iterative decoders employed by the two-hop relay-aided system, we use two EXIT charts [7], [8] to examine the evolution of the input/output

mutual information exchanges between the inner amalgamated "STBC_s-URC_s" decoder and the outer IRCC_s decoder at the relay node and between the parallel amalgamated "STBC_s-URC_s-IRCC_s" decoder and the amalgamated "STBC_r-IRCC_r" decoder at the destination node during the consecutive iterations. As has been investigated in [22] and [23], a narrow but marginally open EXIT tunnel between the EXIT curves of the inner amalgamated "STBC_s-URC_s" decoder and the outer IRCC_s decoder at the relay node indicates that a performance close to the capacity of the source-to-relay link could be achieved. Similarly, at the destination node, a narrow-but-open EXIT tunnel between the EXIT curves of the parallel amalgamated "STBC_s-URC_s-IRCC_s" decoder and the amalgamated "STBC_r-IRCC_r" decoder indicates the possibility of achieving decoding convergence to an infinitesimally low bit error ratio (BER) at SNRs close to the relay channel's capacity. Therefore, we propose a joint source-and-relay mode design procedure to support near-capacity cooperative communications and to maximize the system's effective throughput, which can be simplified to two EXIT-curve-matching problems summarized as follows.

- Step 1) Choose a specific average code rate R_s for the IRCC_s at the source node, and employ the EXIT-curve-matching algorithm of [12] to obtain the optimized weighting coefficients α_i , $i = 1, \dots, 17$ of IRCC_s, where a narrow but marginally open EXIT tunnel between the EXIT curves of the inner amalgamated "STBC_s-URC_s" decoder and the outer IRCC_s decoder emerges at the relay node. This implies that a near-capacity performance may be achieved for the source-to-relay communication link. Then, we store the value of the corresponding transmit power required at the source node.
- Step 2) Choose the same transmit power at the source as stored in Step 1). Fix the optimized weighting coefficients α_i , $i = 1, \dots, 17$, of the IRCC_s obtained in Step 1) at the source node; perform iterative decoding by exchanging extrinsic information between the amalgamated "STBC_s-URC_s" decoder and the IRCC_s decoder during *Phase I* at the destination node, until the further increase in the area A_E under the EXIT curve of the amalgamated "STBC_s-URC_s-IRCC_s" decoder becomes marginal; and then, stop this "inner" iterative decoding process.
- Step 3) Assume perfectly error-free DF relaying and the same transmit power at the relay as that of the source in the second EXIT chart, which examines the evolution of the input/output mutual information exchanges in the three-stage iterative decoder of the Ir-DST coding scheme. Use the EXIT-curve-matching algorithm of [12] to match the SNR-dependent EXIT curve of the amalgamated "STBC_r-IRCC_r" decoder to the target EXIT curve of the amalgamated "STBC_s-URC_s-IRCC_s" decoder observed in Step 2). Obtain the maximized average code rate R_r and the optimized weighting coefficients β_j , $j = 1, \dots, 17$ of IRCC_r when a narrow-but-open EXIT tunnel emerges.

In this paper, we consider an average code rate of $R_s = 0.5$ for the outer IRCC_s at the source node and the specific relay network configuration with $G_{sr} = 8$ and $G_{rd} = 2$, which satisfies (5). The EXIT chart of the serially concatenated IRCC_s-URC_s-STBC_s scheme of the source-to-relay link is shown in Fig. 5, where the decoding trajectories are computed based on a frame length of 250 000 bits. The EXIT curve of the outer IRCC_s having optimized weighting coefficients α_i , as shown in Fig. 5, was constructed using the curve-matching algorithm of [12]. As we can see from Fig. 5, a narrow but marginally open EXIT tunnel emerges for the 2×2 source-to-relay communication

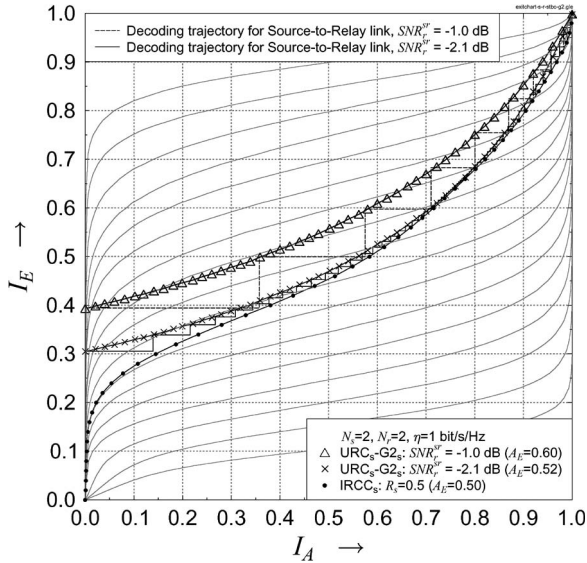


Fig. 5. EXIT chart curves of the URC_s-G2_s, the IRCC_s with optimized weighting coefficients $[\alpha_1, \dots, \alpha_{17}] = [0, 0, 0, 0, 0, 0.327442, 0.186505, 0.113412, 0, 0.0885527, 0, 0.0781214, 0.0962527, 0.0114205, 0.0346015, 0.0136955, 0.0500168]$, and 17 IRCC subcodes for the 2×2 source-to-relay communication link.

link. A receive SNR of about -2.1 dB is needed to attain a decoding convergence to an infinitesimally low BER. Due to the geometrical gain of the source-to-relay link, the equivalent SNR⁵ at the source node can be computed as

$$\text{SNR}_e^s = \text{SNR}_e^{sr} - 10 \log_{10}(G_{sr}) [\text{in decibels}] \quad (19)$$

where SNR_e^{sr} is the receive SNR at the relay node. Hence, the minimum SNR_e^s at the source node required for the sake of obtaining a near-error-free performance at the relay node is -11.1 dB. As presented in Section II, we assume that both the source and the relay transmit their signals at the same transmit power; hence, they have the same equivalent SNR. To avoid the potentially high computational complexity at the relay node, a wider-than-necessary EXIT tunnel is created in the EXIT chart in Fig. 5 at the receive SNR of -1.0 dB at the relay node, which corresponds to an equivalent SNR of -10 dB based on (19) at both the source and relay nodes. As can clearly be seen in the EXIT chart in Fig. 6 at the destination node, after five “inner” iterations between the IRCC_s decoder and the amalgamated “STBC_s-URC_s” decoder, the increase in the area A_E under the amalgamated “STBC_s-URC_s-IRCC_s” decoder becomes marginal. Hence, we fix the number of “inner” iterations to $I_i^d = 4$ at the destination node. Following the aforementioned design procedure, we obtain the resultant matching EXIT curve for the Ir-DST coding scheme in Fig. 6, where the IRCC_r has the optimized weighting coefficients β_j and a maximized average code rate of $R_r = 0.5$; hence, $L_s = L_r$. It is clearly seen in Fig. 6 that a narrow-but-open EXIT tunnel emerges, which indicates the possibility of achieving decoding convergence to an infinitesimally low BER at near-capacity SNRs for the Ir-DST coding scheme. This prediction is verified in Fig. 6 by plotting the corresponding Monte Carlo simulation-related decoding trajectory, which indeed reaches the (1.0,1.0) point of the EXIT chart. On the other hand, since the code rate R_r of the relay’s IRCC has been maximized by the joint source-and-relay mode design procedure, the

⁵Here, we introduced the terminology of equivalent SNR_e to define the ratio of the signal power at the transmitter side with respect to the noise level at the receiver side, i.e., $\text{SNR}_e = P_0/N_0$, as in [14]. Although this does not have a direct physical interpretation, it simplifies our discussions.

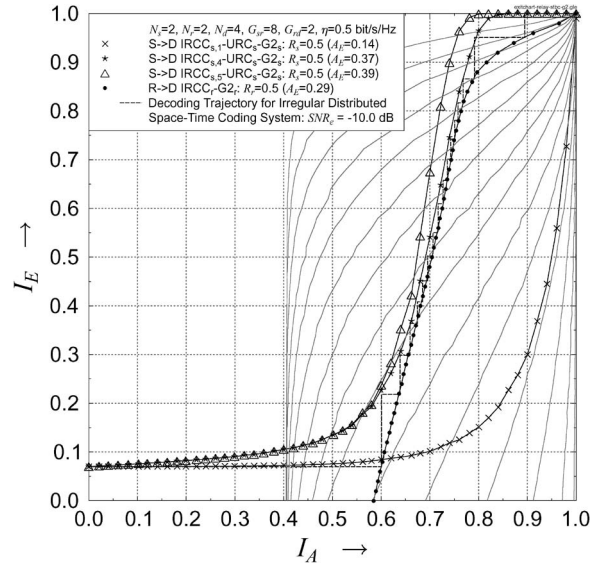


Fig. 6. EXIT chart curves for the IRCC_s-URC_s-G2_s with various “inner” iterations, the IRCC_r-G2_r with IRCC_r having optimized weighting coefficients $[\beta_1, \dots, \beta_{17}] = [0, 0, 0, 0, 0.223115, 0.0158742, 0.292084, 0.220065, 0.0151108, 0, 0, 0, 0, 0, 0, 0.22375]$, and 17 SNR-dependent IRCC_r-G2_r subcodes. The subscript of IRCC_s denotes the number of “inner” iterations between the IRCC_s and “G2_s-URC_s” decoders, and the SNR_e represents the equivalent SNR at both the source and relay nodes.

Ir-DST coding scheme achieves a maximum effective throughput of $(L_s/L_s + L_r)R_s \log_2 4 = 0.5$ bit/s/Hz when the 4QAM-modulated G2 scheme is employed.

V. SIMULATION RESULTS AND DISCUSSIONS

In this section, we present the BER versus equivalent SNR performance of both the perfect and imperfect relaying-aided Ir-DST schemes and that of a noncooperative serially concatenated IRCC-URC-STBC scheme in Fig. 7. For the Ir-DST coding scheme, according to the trajectory predictions shown in Figs. 5 and 6, the number of decoding iterations between the IRCC_s decoder and the amalgamated “STBC_s-URC_s” decoder was fixed to $I^r = 13$ at the relay node. At the destination node, the number of “inner” decoding iterations was fixed to $I_i^d = 4$, whereas the number of “outer” decoding iterations between the parallel amalgamated “STBC_s-URC_s-IRCC_s” decoder and the amalgamated “STBC_r-IRCC_r” decoder was fixed to $I_o^d = 17$. On the other hand, for the noncooperative IRCC-URC-STBC scheme, we employ an outer IRCC, which has the same weighting coefficients α_i and, hence, the same code rate as those of the IRCC_s in the cooperative system. The number of decoding iterations exchanging extrinsic information between the outer IRCC decoder and the inner “STBC-URC” decoder was also fixed to $I_{non} = 13$.

As shown in Fig. 7, the Ir-DST coding scheme outperforms the noncooperative IRCC-URC-STBC scheme by approximately 5.1 dB in terms of the required equivalent SNR, which corresponds to a 3-dB-lower value of 2.1 dB in terms of E_b/N_0 due to a factor-0.5 multiplexing loss in the half-duplex Ir-DST scheme. On the other hand, the performance of the perfect relaying-aided Ir-DST scheme matches the EXIT chart predictions in Fig. 6, whereas the imperfect relaying-aided Ir-DST coding scheme performs similarly to the perfect relaying scheme. This is due to the fact that the source information becomes near error free at the relay node after a sufficiently high number of decoding iterations. Furthermore, it is clearly shown in Fig. 7 that the Ir-DST coding scheme is capable of performing within 1.4 dB of the corresponding relay channel’s DCMC capacity.

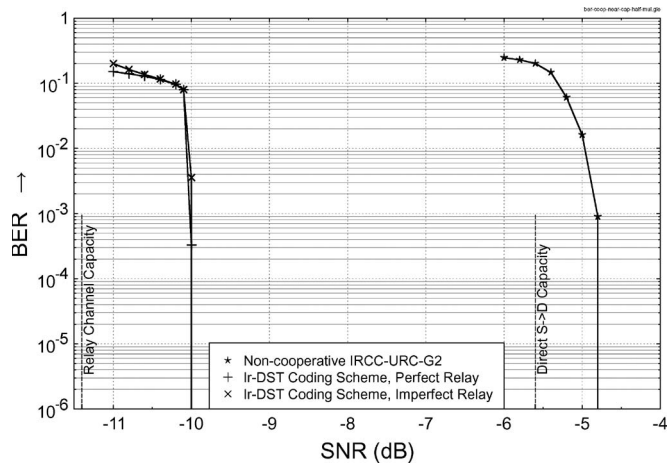


Fig. 7. BER versus equivalent SNR performance of both perfect and imperfect relaying Ir-DST and noncooperative IRCC-URC-G2 schemes for a frame length of 250 000 bits, where the cooperative network is configured with $G_{sr} = 8$, $G_{rd} = 2$, and $L_s = L_r$, and the noncooperative system is equipped with two transmit and four receive antennas.

VI. CONCLUSION

In this contribution, we have proposed an Ir-DST coding scheme for near-capacity cooperative communications. We have derived the CCMC capacity and the constrained information-rate bounds of Alamouti's G2 scheme for the half-duplex relay channel. The proposed joint source-and-relay mode design procedure is capable of finding the optimal Ir-DST coding scheme, which performs close to the capacity limit and achieves a maximum effective throughput. Furthermore, the code-design procedure is not limited to a specific networking scenario; it is applicable under virtually any network configuration.

REFERENCES

- [1] A. Sendonaris, E. Erkip, and B. Aazhang, "User cooperation diversity: Part I and II," *IEEE Trans. Commun.*, vol. 51, no. 11, pp. 1927–1948, Nov. 2003.
- [2] J. Laneman, D. Tse, and G. Wornell, "Cooperative diversity in wireless networks: Efficient protocols and outage behavior," *IEEE Trans. Inf. Theory*, vol. 50, no. 12, pp. 3062–3080, Dec. 2004.
- [3] J. Laneman and G. Wornell, "Distributed space-time-coded protocols for exploiting cooperative diversity in wireless networks," *IEEE Trans. Inf. Theory*, vol. 49, no. 10, pp. 2415–2425, Oct. 2003.
- [4] K. Azarian, H. El Gamal, and P. Schniter, "On the achievable diversity-multiplexing tradeoff in half-duplex cooperative channels," *IEEE Trans. Inf. Theory*, vol. 51, no. 12, pp. 4152–4172, Dec. 2005.
- [5] B. Zhao and M. Valenti, "Distributed turbo coded diversity for relay channel," *Electron. Lett.*, vol. 39, no. 10, pp. 786–787, May 2003.
- [6] S. X. Ng, Y. Li, and L. Hanzo, "Distributed turbo trellis coded modulation for cooperative communications," in *Proc. ICC*, Dresden, Germany, Jun. 14–18, 2009, pp. 1–5.
- [7] S. ten Brink, "Convergence behaviour of iteratively decoded parallel concatenated codes," *IEEE Trans. Commun.*, vol. 49, no. 10, pp. 1727–1737, Oct. 2001.
- [8] S. ten Brink, "Designing iterative decoding schemes with the extrinsic information transfer chart," *AEU Int. J. Electron. Commun.*, vol. 54, no. 6, pp. 389–398, Nov. 2000.
- [9] Z. Zhang and T. Duman, "Capacity-approaching turbo coding for half-duplex relaying," *IEEE Trans. Commun.*, vol. 55, no. 10, pp. 1895–1906, Oct. 2007.
- [10] J. G. Proakis, *Digital Communications*, 4th ed. New York: McGraw-Hill, 2001.
- [11] S. X. Ng and L. Hanzo, "On the MIMO channel capacity of multidimensional signal sets," *IEEE Trans. Veh. Technol.*, vol. 55, no. 2, pp. 528–536, Mar. 2006.

- [12] M. Tüchler and J. Hagenauer, "EXIT charts of irregular codes," in *Proc. 36th Annu. Conf. Inf. Sci. Syst.*, Princeton, NJ, Mar. 2002. [CD-ROM].
- [13] M. Tüchler, "Design of serially concatenated systems depending on the block length," *IEEE Trans. Commun.*, vol. 52, no. 2, pp. 209–218, Feb. 2004.
- [14] H. Ochiai, P. Mitran, and V. Tarokh, "Design and analysis of collaborative diversity protocols for wireless sensor networks," in *Proc. VTC—Fall*, Los Angeles, CA, Sep. 26–29, 2004, pp. 4645–4649.
- [15] A. Host-Madsen and J. Zhang, "Capacity bounds and power allocation for wireless relay channels," *IEEE Trans. Inf. Theory*, vol. 51, no. 6, pp. 2020–2040, Jun. 2005.
- [16] A. Høst-Madsen, "Capacity bounds for cooperative diversity," *IEEE Trans. Inf. Theory*, vol. 52, no. 4, pp. 1522–1544, Apr. 2006.
- [17] S. M. Alamouti, "A simple transmit diversity technique for wireless communications," *IEEE J. Sel. Areas Commun.*, vol. 16, no. 8, pp. 1451–1458, Oct. 1998.
- [18] D. Divsalar, S. Dolinar, and F. Pollara, "Serial turbo trellis coded modulation with rate-1 inner code," in *Proc. ISIT*, Sorrento, Italy, Jun. 25–30, 2000, p. 194.
- [19] L. Hanzo, T. H. Liew, and B. L. Yeap, *Turbo Coding, Turbo Equalisation and Space Time Coding for Transmission Over Wireless channels*. New York: Wiley-IEEE Press, 2002.
- [20] T. M. Cover and A. E. Gamal, "Capacity theorems for the relay channel," *IEEE Trans. Inf. Theory*, vol. IT-25, no. 5, pp. 572–584, Sep. 1979.
- [21] S. X. Ng, S. Das, J. Wang, and L. Hanzo, "Near-capacity iteratively decoded space-time block coding," in *Proc. IEEE VTC—Spring*, Marina Bay, Singapore, May 11–14, 2008, pp. 590–594.
- [22] S. X. Ng, J. Wang, and L. Hanzo, "Unveiling near-capacity code design: The realization of Shannon's communication theory for MIMO channels," in *Proc. ICC*, Beijing, China, May 19–23, 2008, pp. 1415–1419.
- [23] L. Kong, S. X. Ng, and L. Hanzo, "Near-capacity three-stage downlink iteratively decoded generalized layered space-time coding with low complexity," in *Proc. GLOBECOM*, New Orleans, LA, Nov. 30–Dec. 4, 2008, pp. 1–6.

Maximum A Posteriori Approach to Time-of-Arrival-Based Localization in Non-Line-of-Sight Environment

Kenneth W. K. Lui, H. C. So, and W.-K. Ma

Abstract—A conventional approach to mobile positioning is to utilize the time-of-arrival (TOA) measurements between the mobile station (MS) and several receiving base stations (BSs). The TOA information defines a set of circular equations from which the MS position can be calculated with the known BS geometry. However, when the TOA measurements are obtained from the non-line-of-sight (NLOS) paths, the position estimation performance can be very unreliable. Assuming that the NLOS probability and distribution are known and the NLOS-induced error dominates the corresponding TOA measurement, two maximum a posteriori probability (MAP) algorithms for NLOS detection and MS localization are derived in this paper. The first provides a standard MAP solution, while the second is a simplified version based on geometric constraints. It is shown that the former achieves more accurate estimation performance at the expense of higher computational cost.

Index Terms—Mobile positioning, non-line of sight (NLOS), time of arrival (TOA).

Manuscript received May 14, 2009; revised September 16, 2009. First published December 31, 2009; current version published March 19, 2010. This work was supported by the Research Grants Council of the Hong Kong Special Administrative Region, China, under Project CityU 119606. The review of this paper was coordinated by Prof. Y. Ma.

K. W. K. Lui and H. C. So are with the Department of Electronic Engineering, City University of Hong Kong, Kowloon, Hong Kong.

W.-K. Ma is with the Department of Electronic Engineering, Chinese University of Hong Kong, Shatin, Hong Kong.

Color versions of one or more of the figures in this paper are available online at <http://ieeexplore.ieee.org>.

Digital Object Identifier 10.1109/TVT.2009.2039762